The Astronomical Journal, 148:43 (15pp), 2014 September doi:10.1088/0004-6256/148/3/43

TIME ELEMENTS FOR ENHANCED PERFORMANCE OF THE DROMO ORBIT PROPAGATOR

Giulio Baù[1] and Claudio Bombardelli[2]
[1] Postdoctoral Researcher, Department of Mathematics, University of Pisa,
Largo Bruno Pontecorvo 5, I-56127 Pisa, Italy; bagiugio@gmail.com
[2] Research Fellow, Department of Applied Physics, E.T.S.I. Aeronáuticos, Universidad Politécnica de Madrid,
Plaza Cardenal Cisneros 3, E-28040 Madrid, Spain; claudio.bombardelli@upm.es
Received 2014 March 27; accepted 2014 May 26; published 2014 July 22

ABSTRACT

We propose two time elements for the orbit propagator named Dromo. One is linear and the other constant with respect to the independent variable, which coincides with the osculating true anomaly in the Keplerian motion. They are defined from a generalized Kepler's equation written for negative values of the total energy and, unlike the few existing time elements of this kind, are free of singularities. To our knowledge it is the first time that a constant time element is associated with a second-order Sundman time transformation. Numerical tests to assess the performance of the Dromo method equipped with a time element show the remarkable improvement in accuracy for the perturbed bounded motion around the Earth compared to the case in which the physical time is a state variable. Moreover, the method is competitive with and even better than other efficient sets of elements. Finally, we also derive a time element for a null and positive total energy.

Key words: celestial mechanics – methods: numerical

1. INTRODUCTION

An important and powerful tool in celestial mechanics is represented by the differential transformation of the physical time t to a new independent variable s, sometimes called fictitious time, as given by:

$$\mathrm{d}t = c\, r^{\alpha} \mathrm{d}s, \tag{1}$$

with c in general being a function of the position and velocity, r the orbital radius, and α a positive real number.

The above transformation is sometimes called a "generalized Sundman transformation" of α order following the work of the Finnish astronomer Carl Sundman in 1912, who succeeded in the exclusion of binary collisions in the three-body problem by means of Equation (1) with c and α both equal to one.[3] In this way he derived a series expansion for the coordinates of the three bodies valid for all time (Siegel & Moser 1971, Chapter 1).

The benefits brought by the employment of time transformations are many and include a performance increase in the numerical propagation of the orbital motion under the Newtonian attraction of a central body and a small perturbation. This comes as a result of several factors.

First of all, they can reduce or eliminate the Lyapunov instability of the unperturbed elliptical two-body problem (Stiefel & Scheifele 1971, p. 75; Bond 1982), as shown by Baumgarte (1972) and Velez (1974), with a consequent reduction of the global numerical integration error. Secondly, they produce an analytic regulation of the integration step size (Stiefel & Scheifele 1971, pp. 77–78), with a consequent uniformization and reduction of the local truncation error over one orbital revolution (Velez 1974; Feagin & Mikkilineni 1976; Velez & Hilinski 1978). Such uniformization has the important advantage of allowing the use of fixed step size numerical methods even in the numerical integration of highly eccentric orbits (Janin 1974; Velez 1974) thus avoiding resorting to more sophisticated, and in some cases less efficient, variable step size schemes.

Further discussions and references about the aspects of stabilization, uniformization of the local truncation error, and numerical error propagation related to the usage of a time transformation in the perturbed two-body problem can be found in Nacozy (1976a).

As a consequence of changing the independent variable, Equation (1) is added to the system of differential equations with physical time becoming a new state variable. Such an equation may exhibit dynamical instability itself depending on the value of the exponent α. As noted by Velez (1974), the benefit of the time stabilization of the Newtonian equations of motion can be significantly deteriorated by the numerical error of the physical time. This deleterious effect will be higher when time appears explicitly inside the perturbative terms and is still present in the case of time-independent perturbations whenever the position is required at specific epochs.

Numerical results have shown that the local truncation error associated with physical time, and therefore the global error of the state vector, can be reduced with the introduction of new state variables called *time elements*. A time element was first defined by Stiefel and Scheifele as "any quantity which, during a pure Kepler motion, is a linear function of the independent variable" (Stiefel & Scheifele 1971, p. 83). Two well-known examples of time elements are given by the time of pericenter passage and the mean anomaly in relation to the physical time. In practice, one common way of introducing a time element is to analytically integrate Equation (1) in the unperturbed case for the selected values of c and α. As a result, a relation between the time and the time element can be established, and by exploiting methods of variation of parameters, the differential equation of the time element is derived for the perturbed motion.

The research of time elements to be employed in the numerical computation of orbits started at the end of the 1960s and continued mainly until the beginning of the 1980s. In the literature, two kinds of time elements appear depending on whether they are *constant* (i.e., the time element is a prime integral)

[3] One should note that the same time transformation had been adopted a few years before by the Italian mathematician Tullio Levi-Civita (1906) together with a change of the spatial variables for regularizing the restricted three-body problem.

or *linear* in Keplerian motion with respect to the independent variable (s). As pointed out by Nacozy (1976b), these time elements differ according to two features. Linear time elements lead to differential equations that are free of secular terms, hence avoiding the quadratic growth of the local truncation error. On the other hand, constant time elements are affected by a much smaller local truncation error.

Stiefel & Scheifele (1971, Section 18) develop a linear time element with respect to the independent variable for the Kustaanheimo–Stiefel (K-S) regularization and report of the increased accuracy in the computation of time as observed by numerical experiments (see also Velez 1974). As recently discovered by Fukushima (2005), the reason for the improvement lies in a change of the error growth of the physical time from quadratic to linear associated with this time element. The Stiefel–Scheifele time element has also been proposed in combination with the Newtonian equations of motion (Baumgarte 1972; Baumgarte & Stiefel 1974). Numerical tests show that the integration of the stabilized equations in Cartesian coordinates equipped with a time element can be as accurate as a regularized set of elements (Janin 1974). An interesting property of the Stiefel–Scheifele time element is that it can be incorporated as a coordinate into several canonical sets of variables by means of a canonical transformation applied in the extended phase space (Ferrándiz & Sansaturio 1995).

Another key contribution to the research of time elements for time transformations (1) is found in the work of Nacozy, who explores three different linear time elements related to the eccentric ($\alpha = 1$), true ($\alpha = 2$), and intermediate ($\alpha = 3/2$) anomalies, respectively (Nacozy 1981). Because the definition given by Nacozy stems from Kepler's equation in its classic form, the differential equations result in cumbersome expressions that contain the semi-major axis, eccentricity, and the anomalies. By writing Kepler's equation in terms of the state vector and the Keplerian energy (as done in Stiefel & Scheifele 1971), Kwok & Nacozy (1981) obtain much more compact derivatives of the Nacozy's time elements wherein the position and velocity appear explicitly. One order of magnitude in the accuracy of the position is gained by the three time elements with respect to the integration of Equation (1). Numerical devices to further increase the accuracy are discussed in Nacozy (1976b). It is worth noting that while the time element related to $\alpha = 1$ is the already known Stiefel–Scheifele time element applied to the Newtonian equations, as far as we know, Nacozy is the first to propose time elements for the true and intermediate anomalies.

More recent work on linear time elements associated with a generalized Sundman transformation with $\alpha = 2$ is found in a series of papers by Ferrándiz et al. A time element is attached to the Burdet–Ferrándiz (B-F) focal variables in Ferrándiz & Sansaturio (1990). The definition is obtained by applying a similar technique employed by Nacozy (1981) but with two key differences. First, Kepler's equation is considered in a generalized form where the total energy replaces the Keplerian energy, and second, the time element is proportional to the independent variable while Nacozy's is proportional to the osculating true anomaly, the two angles coinciding only in the case of unperturbed motion. The benefit of this time element for the numerical integration of the perturbed motion along highly eccentric orbits is analyzed in three papers by Ferrándiz et al. (1991, 1992b, 1993). A sensitive decrease of the accumulated position error under the J_2 perturbation is seen when compared to the original B-F method where the physical time is integrated. Furthermore, the improvement brought by the use of a time element in B-F focal variables is much more significant than for the corresponding K-S regularization whose performance is only slightly improved by a time element. This advantage increases for higher eccentricities and still holds for long-term integrations. Time-dependent perturbations deteriorate the efficiency of the method, especially with a fixed step size numerical integrator; nonetheless, when compared with many other formulations, it continues to show the best behavior with a variable step size scheme.

The constant generated by the analytic integration of the time transformation can be selected as a time element, which, in this case, takes the physical interpretation of the time of passage through a certain point along the orbit. Burdet (1968) (see also Bond & Allman 1996, Section 9) develops a set of elements linked to the spatial variables of Sperling's regularization together with four temporal integrals in place of the physical time. The time element is one of these integrals and it represents the initial time, while the other three are functions of the spatial elements. Bond (1974) includes the same time element as Burdet in the uniform and regular elements for the K-S method and shows that the overabundant integrals for computing the time eliminate the mixed secular terms from the derivative of the time element with a consequent improvement in efficiency.

The time of pericenter passage is employed as a time element associated with a time transformation of the type given in Equation (1) in two works. Baumgarte (1976) introduced it in conjunction with a general time transformation, but two drawbacks discourage its use: the singularity for circular orbits and the presence of the multi-value arctangent function. The latter was circumvented by adding a stabilized differential equation for the time. Then, more recently Arakida & Fukushima (2001) inserted it into the framework of the element method proposed by Stiefel in 1967 for the K-S regularization.

In this paper, we define and test two time elements for a special perturbation method (Baù et al. 2013) that relies on a generalized Sundman time transformation of the form shown in Equation (1) with the exponent α set equal to 2. The method, called Dromo(P), represents a generalization of the original formulation published by Peláez et al. (2007) for taking advantage of perturbations deriving from a potential. The state of the propagated particle is described by means of the physical time and seven generalized orbital elements that are strictly related to the variables of the B-F linearization, namely the inverse of the orbital radius and the unit vector of the position. Originally introduced by Burdet (1969) and later by Ferrándiz (1988) and Ferrándiz et al. (1992a) as canonical coordinates, they transform the two-body problem into four harmonic oscillators with unit frequency when the independent variable obeys Equation (1) wherein $\alpha = 2$ and c is the inverse of the angular momentum per unit mass.

The motivation of our work comes from the results of the analysis done by Ferrándiz on the numerical behavior of the B-F regularization. In Ferrándiz et al. (1992a), it is shown that for highly eccentric orbits perturbed by the J_2 zonal harmonic of Earth's gravity field, the step size is completely driven by the integration of the physical time. This interesting feature, which is not observed in the K-S regularization, suggests that a time element can be very effective in the B-F method, at least when the perturbation does not explicitly depend on the physical time. This is in line with results shown in Baù et al. (2013) in relation to the Dromo(P) method.

The equations for implementing the first time element in the framework of the Dromo(P) method are obtained in Section 2. From the generalized Sundman time transformation, a quadrature yields the generalized version of Kepler's equation, which is modified to introduce a linear time element in the independent variable. After a direct differentiation, the derivative of the time element is determined. The resulting time element is not affected by singularities which instead appear in similar time elements presented in the literature. With just a little effort, an alternative time element, which is a constant in the unperturbed motion, is also developed. As far as we know, it represents the first example of a constant time element relative to a time transformation (1) with $\alpha = 2$, which is not affected by the limitation due to the multi-value arctangent function. Both time elements are presented for a negative total energy and we address the case of positive and null energy in Appendix B.

In Section 3, using the support of numerical examples, we corroborate the usefulness of completing the Dromo(P) set of elements with a time element. By restricting the problem to the perturbed motion around the Earth, we monitor two performance metrics: the accuracy achieved at a given epoch corresponding to a few tens of revolutions and the position and time error accumulated throughout thousands of revolutions. Both conservative and time-dependent perturbations are applied with different initial eccentricities. As a first goal, we propose showing the improvement caused in Dromo(P) when the spatial elements are equipped with the time elements described in this paper as opposed to the physical time as in Baù et al. (2013). Finally, we compare the performance of the eight generalized orbital elements of Dromo(P) with respect to other efficient and popular sets of elements.

Non-dimensional quantities are used throughout this paper. For the reference length, we use the orbital distance at the initial epoch, for the reference time, we use the inverse of the mean motion of a circular orbit with a radius equal to the reference length, and for the reference mass, we use the mass of the propagated body.

2. TWO TIME ELEMENTS RELATED TO THE TIME OF PERICENTER PASSAGE

The two proposed time elements are developed in the framework of the spatial variables of Dromo(P) which are recalled below.

2.1. The Spatial Variables of the Dromo(P) Method

Let $\boldsymbol{r}$ and $\boldsymbol{v}$ be the position and velocity vectors of the propagated body relative to a central body. The particle is acted upon by the gravitational attraction of the central body and a perturbing force that is regarded as the sum of two contributions:

$$\boldsymbol{F} = -\frac{\partial\, \mathcal{U}\,(t,\, \boldsymbol{r})}{\partial\, \boldsymbol{r}} + \boldsymbol{P}, \tag{2}$$

where $\mathcal{U}$ is the disturbing potential energy and $\boldsymbol{P}$ includes those perturbations that do not arise from a potential $\mathcal{U}$.

Dromo is a formulation of the perturbed two-body problem that describes the motion by means of the physical time and seven spatial elements, which are constants in the Keplerian case. In its most recent version (Baù et al. 2013), referred to as Dromo(P), a generalized Sundman transformation relates the time t to the new independent variable ϕ:

$$\frac{\mathrm{d}t}{\mathrm{d}\phi} = \frac{r^2}{c}, \tag{3}$$

where here c ($\tilde{h}$ in Baù et al. 2013) is called the generalized angular momentum and reads:

$$c = \sqrt{h^2 + 2\, r^2\, \mathcal{U}}, \tag{4}$$

with $h = |\boldsymbol{r} \times \boldsymbol{v}|$ being the orbital angular momentum and $r = |\boldsymbol{r}|$ the orbital radius. As detailed in Baù et al. (2013), c can be obtained from the angular momentum definition by formally replacing the Keplerian energy ε_K with the total energy $\varepsilon = \varepsilon_K + \mathcal{U}$.

In a similar fashion, one can introduce the generalized eccentricity g as:

$$g = \sqrt{1 + 2\, \varepsilon\, c^2}, \tag{5}$$

and the generalized true anomaly θ, univocally defined in the range $[0,\ 2\pi)$ by:

$$g\, \sin\theta = c\, \frac{\mathrm{d}r}{\mathrm{d}t}, \qquad g\, \cos\theta = \frac{c^2}{r} - 1. \tag{6}$$

It can be readily verified that, for the case in which $\mathcal{U} = 0$, the generalized quantities c, θ, and g coincide with the osculating angular momentum, true anomaly, and eccentricity, respectively.

The first two spatial Dromo(P) elements are defined as (see Equations (52) and (53) on p. 65 of Baù et al. 2013):

$$\zeta_1 = \left(\frac{c}{r} - \frac{1}{c}\right) \cos\phi + \frac{\mathrm{d}r}{\mathrm{d}t}\, \sin\phi, \tag{7}$$

$$\zeta_2 = \left(\frac{c}{r} - \frac{1}{c}\right) \sin\phi - \frac{\mathrm{d}r}{\mathrm{d}t}\, \cos\phi. \tag{8}$$

These equations can now be written in a more compact form by employing Equation (6) to eliminate the terms r and $\mathrm{d}r/\mathrm{d}t$:

$$\zeta_1 = \frac{g}{c} \cos\left(\phi - \theta\right), \tag{9}$$

$$\zeta_2 = \frac{g}{c} \sin\left(\phi - \theta\right). \tag{10}$$

The angle:

$$\gamma = \phi - \theta \tag{11}$$

has an important physical interpretation which is explained in the following. Let us first introduce the orbital frame orthonormal basis $(\boldsymbol{i},\ \boldsymbol{j},\ \boldsymbol{k})$:

$$\boldsymbol{k} = \frac{\boldsymbol{r} \times \boldsymbol{v}}{h}, \qquad \boldsymbol{i} = \frac{\boldsymbol{r}}{r}, \qquad \boldsymbol{j} = \boldsymbol{k} \times \boldsymbol{i}, \tag{12}$$

and consider a generic perturbation $\boldsymbol{F}$:

$$\boldsymbol{F} = R\, \boldsymbol{i} + T\, \boldsymbol{j} + N\, \boldsymbol{k}.$$

Next, let us introduce the generalized eccentricity vector:

$$\boldsymbol{g} = -\boldsymbol{i} + \boldsymbol{w} \times \boldsymbol{c}, \tag{13}$$

where the generalized velocity and angular momentum vectors obey:

$$\boldsymbol{w} = \frac{\mathrm{d}r}{\mathrm{d}t}\, \boldsymbol{i} + \frac{c}{r}\, \boldsymbol{j}, \qquad \boldsymbol{c} = c\, \boldsymbol{k}. \tag{14}$$

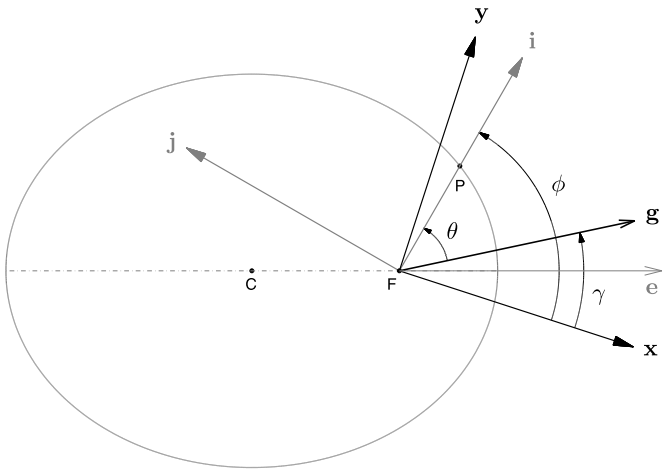

Figure 1. Axes $\boldsymbol{x}$ and $\boldsymbol{y}$ of the intermediate reference frame as viewed from the $\boldsymbol{k}$ axis (Equation (12)). The propagated body occupies the position P along an osculating ellipse with the center in C, one focus in F, and the eccentricity vector indicated by $\boldsymbol{e}$. The elements ζ_1 and ζ_2 of the Dromo(P) formulation are the projections of the generalized eccentricity vector $\boldsymbol{g}$ (Equation (13)) along $\boldsymbol{x}$ and $\boldsymbol{y}$, respectively.

After substituting the above expressions into Equation (13) and taking into account Equation (6) we have:

$$\boldsymbol{g} = g\,(\boldsymbol{i}\,\cos\theta - \boldsymbol{j}\,\sin\theta)\,. \tag{15}$$

Moreover, Equations (9) and (10) invite one to introduce two orthogonal unit vectors, $\boldsymbol{x}$ and $\boldsymbol{y}$, lying on the orbital plane such that:

$$\boldsymbol{g} = c\,(\zeta_1\,\boldsymbol{x} + \zeta_2\,\boldsymbol{y}) = g\,(\boldsymbol{x}\,\cos\gamma + \boldsymbol{y}\,\sin\gamma)\,. \tag{16}$$

Let us compose the basis $(\boldsymbol{x},\ \boldsymbol{y},\ \boldsymbol{z})$ and call it the intermediate frame (analogous to the *ideal* frame—as it was originally called by the astronomer P. A. Hansen in 1857—employed by Deprit 1975). We deduce from Equations (15) and (16) that the unit vectors $\boldsymbol{x}$ and $\boldsymbol{y}$ are obtained from $\boldsymbol{i}$ and $\boldsymbol{j}$ by a rotation of ϕ around the axis associated with $\boldsymbol{k}$ as shown in Figure 1[4]:

$$\begin{aligned}\boldsymbol{x} &= \boldsymbol{i}\,\cos\phi - \boldsymbol{j}\,\sin\phi,\\ \boldsymbol{y} &= \boldsymbol{i}\,\sin\phi + \boldsymbol{j}\,\cos\phi.\end{aligned}$$

It follows that the angular velocity $\boldsymbol{\omega}_{\mathcal{I}}$ of the intermediate frame with respect to a *fixed* frame is the composition of a rotation from the fixed frame to the orbital frame with an angular velocity $\boldsymbol{\omega}_{\mathcal{O}}$ (see Equation (14) on p. 3 of Deprit 1975) and a rotation from the orbital frame to the intermediate frame with the angular velocity $\boldsymbol{\omega}_{\mathcal{IO}} = -(\mathrm{d}\phi/\mathrm{d}t)\,\boldsymbol{k}$:

$$\boldsymbol{\omega}_{\mathcal{I}} = \boldsymbol{\omega}_{\mathcal{O}} + \boldsymbol{\omega}_{\mathcal{IO}} = N\,\frac{r}{h}\,\boldsymbol{i} + \frac{h-c}{r^2}\,\boldsymbol{k}. \tag{17}$$

Equations (15) and (16) show that the angles ϕ and γ describe, respectively, the angular position of the particle P and the rotation of the generalized eccentricity vector $\boldsymbol{g}$ with respect to the vector $\boldsymbol{x}$ of the intermediate frame. In the case of pure Keplerian motion, $\boldsymbol{g}$ becomes the eccentricity vector $\boldsymbol{e}$ and γ represents the orientation of the line of apsides with respect to the axis associated with $\boldsymbol{x}$, which is fixed according to Equation (17). If only the perturbation $\boldsymbol{P}$ is present, that is $\mathcal{U} = 0$, γ still measures the angular displacement of $\boldsymbol{e}$ reckoned from $\boldsymbol{x}$ but it is not a constant since both the directions of $\boldsymbol{e}$ and $\boldsymbol{x}$ are affected by $\boldsymbol{P}$. As shown in Appendix II of Baù et al. (2013), γ can be expressed as ($\mathcal{U} = 0$):

$$\gamma = \omega - \omega_0 + \int_{\Omega_0}^{\Omega} \cos i\,\mathrm{d}\kappa, \tag{18}$$

where ω, Ω, and i are the argument of pericenter, the longitude of the ascending node, and the inclination of the osculating orbit. Also note that when the out-of plane component of $\boldsymbol{P}$ is zero, then $\boldsymbol{x}$ is fixed (as can be seen from Equation (17)) together with the orientation of the orbital plane, and as predicted by Equation (18), γ is simply equal to the variation of ω with respect to its initial value ω_0. Such a straightforward interpretation of γ and, in turn, of ζ_1 and ζ_2 has been exploited in two recent papers by Bombardelli et al. (2011, 2012) to develop a perturbation theory for the orbit propagation of a point mass perturbed by a constant tangential thrust.

The spatial orbital elements ζ_4, ζ_5, ζ_6, and ζ_7 are the components of a unit quaternion ζ that describes the orientation of the intermediate frame except for a constant rotation ϕ_0 around the $\boldsymbol{k}$ axis. More precisely, if we indicate with $(\boldsymbol{x}_0,\ \boldsymbol{y}_0,\ \boldsymbol{k})$ the reference frame associated with ζ then we have:

$$\boldsymbol{x}_0 = \boldsymbol{x}\,\cos\phi_0 + \boldsymbol{y}\,\sin\phi_0, \qquad \boldsymbol{y}_0 = -\boldsymbol{x}\,\sin\phi_0 + \boldsymbol{y}\,\cos\phi_0,$$

where ϕ_0 is the value taken by ϕ at the initial time $t = 0$. The inertial orientation of the orbital frame can be determined from the intermediate frame by an additional rotation of $\phi - \phi_0$ in the common direction identified by $\boldsymbol{k}$.

Finally, the remaining element, ζ_3, is defined as:

$$\zeta_3 = \frac{1}{c}. \tag{19}$$

As we pointed out at the end of Section 4 in Baù et al. (2013), the total energy should be preferred as a dependent variable instead of ζ_3 whenever a disturbing potential $\mathcal{U}$ is applied.

In summary, the variables ζ_1, ζ_2, and ζ_3 describe the dynamics in the *orbital* frame and ζ_4, ζ_5, ζ_6, and ζ_7, along with ϕ and ϕ_0, fix the orientation of the orbital frame with respect to a *fixed* frame so that the position and velocity of the propagated body can be computed at any time t.

Equations (9) and (10) are the starting point of our approach to develop a time element for the Dromo(P) method.

2.2. Generalized Kepler's Equation

Equation (6) can be rewritten in the form:

$$r = \frac{c^2}{1 + g\cos\theta}, \qquad \frac{\mathrm{d}r}{\mathrm{d}t} = \frac{g\sin\theta}{c}. \tag{20}$$

From here on, we assume that the total energy is negative, $\varepsilon < 0$, which implies that $0 \leqslant g < 1$ (Equation (5)), while the case $\varepsilon \geqslant 0$ is addressed in Appendix B. Analogous to the generalized quantities previously described, we now introduce the generalized eccentric anomaly, G, as fully defined by:

$$\sin G = \frac{\sqrt{1-g^2}\,\sin\theta}{1 + g\cos\theta}, \qquad \cos G = \frac{g + \cos\theta}{1 + g\cos\theta}. \tag{21}$$

[4] The intermediate frame introduced here would represent the ideal frame in Deprit (1975) if ϕ were defined by the transformation (3) with the angular momentum h in place of its generalized counterpart c. Therefore, the two reference frames coincide if the disturbing potential $\mathcal{U}$ is zero.

The radial distance and its time-derivative (Equation (20)) can be written in terms of G with the aid of the above relations and by exploiting Equation (5) to eliminate the explicit dependency on c:

$$r = \frac{g\cos G - 1}{2\,\varepsilon}, \qquad \frac{\mathrm{d}r}{\mathrm{d}t} = \frac{\sqrt{-2\,\varepsilon}\, g \sin G}{1 - g\cos G}. \tag{22}$$

In the case where the generalized eccentricity and total energy are constant in time, which includes unperturbed motion as a particular case, the former equation is differentiated with respect to time and with the help of the latter we find that the differentials of t and G obey:

$$\mathrm{d}t = \frac{r}{\sqrt{-2\,\varepsilon}}\,\mathrm{d}G, \tag{23}$$

where r is a function of G. Finally, the integration of Equation (23) yields the generalized Kepler's equation:

$$t = \tau_p + \frac{1}{(-2\,\varepsilon)^{3/2}}\left(G - g\sin G\right), \tag{24}$$

where τ_p can be regarded as a generalized time of pericenter passage.

2.3. "Linear" Time Element ζ_0

In the Dromo(P) method, the variable time is obtained by the numerical integration of Equation (3). Here we introduce a time element to be used in place of the physical time. Let us define the quantity:

$$\zeta_0 = \tau_p + \frac{\theta}{(-2\,\varepsilon)^{3/2}}.$$

Because the generalized true anomaly θ differs from ϕ by an arbitrary constant in the absence of perturbations, the element ζ_0 defined above is a linear function of the independent variable for Keplerian motion and can be adopted as a time element in our orbit propagation scheme.

From the generalized Kepler's equation (24) ζ_0 is related to the physical time as:

$$\zeta_0 = t - \frac{1}{(-2\,\varepsilon)^{3/2}}\left(G - \theta - g\sin G\right). \tag{25}$$

We show in Appendix A that the angular difference $G - \theta$ can be expressed in the convenient form:

$$G - \theta = -2\arctan\left(\frac{g\sin\theta}{1 + g\cos\theta + \sqrt{1-g^2}}\right), \tag{26}$$

which is analogous to the relation satisfied by the eccentric and true anomalies (Broucke & Cefola 1973, Equation (1)). It is worth noting that since $g < 1$, the denominator is always positive and therefore $G - \theta$ is a continuous function. As shown by Equation (6), the terms $g\sin\theta$ and $g\cos\theta$ are functions of the orbital radius and radial velocity which, in turn, are computed from (Baù et al. 2013):

$$r = \frac{1}{\zeta_3\, s}, \qquad \frac{\mathrm{d}r}{\mathrm{d}t} = u, \tag{27}$$

where the generalized transverse velocity (s) and the radial velocity (u) obey:

$$s = \zeta_3 + \zeta_1\cos\phi + \zeta_2\sin\phi, \tag{28}$$

$$u = \zeta_1\sin\phi - \zeta_2\cos\phi. \tag{29}$$

From Equations (6) and (27) we obtain the relations:

$$g\sin\theta = \frac{u}{\zeta_3}, \qquad g\cos\theta = \frac{s}{\zeta_3} - 1. \tag{30}$$

The remaining term to work out in Equation (25) is $g\sin G$. By manipulating Equations (22) and performing the substitutions (27) we find:

$$g\sin G = \frac{u\sqrt{-2\,\varepsilon}}{\zeta_3\, s}. \tag{31}$$

Equation (26) along with Equations (5), (19), and (30), and Equation (31) finally allow us to write Equation (25) in the form:

$$\zeta_0 = t - \frac{u}{2\,\varepsilon\,\zeta_3\, s} - \frac{1}{\varepsilon\sqrt{-2\,\varepsilon}}\arctan\left(\frac{u}{s + \sqrt{-2\,\varepsilon}}\right). \tag{32}$$

This equation is a fundamental relation to be used for initializing ζ_0 at $t = 0$ and for updating the time at each integration step (Appendix A contains more details on the implementation of the time element ζ_0 in the Dromo(P) method). Note that the employment of a linear time element has completely avoided the difficulty related to the multi-value arctangent function.

The last necessary step for the use of the variable ζ_0 in an orbit propagation scheme is to relate its derivative to the remaining variables of the method and the perturbing terms. By differentiating Equation (32) with respect to ϕ and after carrying through several algebraic manipulations, which are outlined in Appendix A, the final equation is:

$$\frac{\mathrm{d}\zeta_0}{\mathrm{d}\phi} = a^{3/2}\left[1 + \frac{\mathrm{d}\varepsilon}{\mathrm{d}\phi}\left(6\,a\arctan\left(\frac{u}{f+w}\right) + k_1\right) + \left(\frac{R}{\zeta_3\, s} - 2\,\mathcal{U}\right)k_2\right], \tag{33}$$

where:

$$k_1 = \frac{\sqrt{a}\,u}{s^2}\left(\frac{\zeta_3 + s}{f} + \frac{2\,w}{\zeta_3} + 1\right), \quad k_2 = \frac{1}{s^2}\left(\frac{f}{\zeta_3} + \frac{w}{f} + \frac{u^2}{f\,s}\right), \tag{34}$$

$$a = -\frac{1}{2\,\varepsilon}, \tag{35}$$

$$w = \zeta_1\cos\phi + \zeta_2\sin\phi, \tag{36}$$

$$f = \zeta_3 + \sqrt{-2\,\varepsilon}, \tag{37}$$

s and u are found in Equations (28) and (29), and (Baù et al. 2013):

$$\frac{\mathrm{d}\varepsilon}{\mathrm{d}\phi} = \frac{1}{\zeta_3\, s^2}\left(R_p\, u + T_p\sqrt{s^2 - 2\,\mathcal{U}} + \frac{\partial\,\mathcal{U}}{\partial\, t}\right), \tag{38}$$

with $R_p = \boldsymbol{P}\cdot\boldsymbol{i}$ and $T_p = \boldsymbol{P}\cdot\boldsymbol{j}$.

With regard to the singularities that affect Equations (32) and (33), we see that the only ones are represented by $\zeta_3 = 0$ and $s = 0$ which correspond to an infinite orbital distance and rectilinear motion. The former has little practical significance because we assume that the propagation occurs inside the

sphere of influence of a central body which can possibly be changed if the orbital distance becomes sufficiently large. The latter, inherited by the B-F linearization, represents an unusual dynamical condition for artificial as well as natural bodies.

Time elements related to a time transformation of the kind considered in Equation (1) with $\alpha = 2$ have been developed by just a few authors (see the Introduction). The time elements proposed by Nacozy (1981) and Ferrándiz & Sansaturio (1990) are similar to that presented here, but they both suffer from one more singularity than our time element, which is when the osculating and generalized eccentricities, respectively, are zero. The non-singular nature of the Dromo(P) elements avoids this kind of singularity which can produce a loss of accuracy for near-circular motion.

2.4. "Constant" Time Element τ_0

In Keplerian motion, the time element ζ_0 grows linearly with ϕ at a rate of $a^{3/2}$. This entails the presence, on the right-hand side of the differential Equation (33), of a zero-order term with respect to the perturbation, which may have a dominant contribution to the local truncation error generated by the numerical integration of Equation (33) for weakly perturbed motion. In the end, this would affect the computation of the physical time through Equation (32) and degrade the accuracy of the propagation method as observed by Nacozy (1976b).

In light of these considerations, we seek a time element that behaves like a constant in the unperturbed motion, which would eliminate the leading addend in Equation (33). In the literature we have encountered only a few examples of time elements of this kind (as outlined in the Introduction).

At first sight, one would be tempted to employ the generalized time of pericenter passage τ_p (Equation (24)) as a time element that remains constant in the unperturbed motion. Unfortunately, this approach is doomed to failure since the variable G in the generalized Kepler's equation (24) cannot be properly evaluated from Equation (21) due to the discontinuous multi-value arctangent function. One possible way to partially overcome this difficulty is to compute G from Equation (26) where θ is given by $\phi - \gamma$, as follows from Equation (11). Since we have $\gamma = \mathrm{atan2}\,(\zeta_2,\ \zeta_1)$ (Equations (9) and (10)) one has just shifted the problem to the computation of the angle γ. Even if γ is a slowly varying angle compared with G, a secular drift induced by the perturbations will generate a discontinuity for a sufficiently long propagation time. Notably, Baumgarte (1976) overcomes a similar obstacle at the price of adding a differential equation for the time modified by a control term that depends on the time element.

In this paper, we pursue a different approach. The new time element is defined as:

$$\tau_0 = \zeta_0 - a^{3/2}\,\phi, \tag{39}$$

where a is related to the total energy as shown in Equation (35). By comparison of Equations (24) and (25) and taking into account Equation (39), one finds that $\tau_0 = \tau_p - a^{3/2}\,\gamma$, where γ is the perturbing angle introduced in Equation (11), and as a consequence, τ_0 is a constant in the absence of perturbations. After substituting for ζ_0 in Equation (32), by exploiting Equation (39), we end up with ($\varepsilon < 0$):

$$t = \tau_0 - \frac{a\,u}{\zeta_3\,s} + a^{3/2}\left(\phi - 2\arctan\left(\frac{u}{f+w}\right)\right), \tag{40}$$

where w and f are given in Equations (36) and (37). The derivative of τ_0 with respect to ϕ is easily determined by differentiating Equation (39) with the help of Equations (33), (35), and (38) to yield:

$$\frac{\mathrm{d}\tau_0}{\mathrm{d}\phi} = a^{3/2}\left[\frac{\mathrm{d}\varepsilon}{\mathrm{d}\phi}\left(6\,a\arctan\left(\frac{u}{f+w}\right) - 3\,a\,\phi + k_1\right) + \left(\frac{R}{\zeta_3\,s} - 2\,\mathcal{U}\right)k_2\right], \tag{41}$$

where k_1 and k_2 are provided in Equation (34). As expected, the right-hand side vanishes in the two-body problem. Unlike ζ_0, the local truncation error of τ_0 is scaled by the perturbations and the contribution of τ_0 to the physical time is much smaller compared with the sum of the other terms in Equation (40). However, the derivative of τ_0 exhibits a secular growth as long as non-conservative perturbations are applied, which induces a quadratic increase in the error. By contrast, the rate of change of ζ_0 shown in Equation (33) is periodic and a linear evolution of the error is expected.

For their complementary features, one may think to start the orbit propagation with τ_0 up to a selected number of revolutions to then switch to ζ_0, through Equation (39), which is more recommended for long-term propagations.

In the next section, we combine τ_0 and ζ_0 with the seven spatial elements of Dromo(P) and test the resulting formulations.

3. NUMERICAL EXPERIMENTS

The time elements ζ_0 (Equations (32) and (33)) and τ_0 (Equations (40) and (41)) are applied here, in combination with the spatial variables of the Dromo(P) method, to a series of benchmark orbital propagation problems. The resulting formulations, which are based on eight generalized orbital elements, are compared with the original Dromo(P) method as presented in Baù et al. (2013) in order to investigate the effect of the time elements with respect to the direct employment of the physical time.

We have conducted numerical experiments considering perturbed motion around the Earth. In particular, we are interested in two performance indicators: the computational cost required to achieve a certain level of accuracy in the position, and the accumulation of the error in the position and time in function of the independent variable.

3.1. Benchmark Problems and Compared Methods

The analysis is aimed at assessing the numerical behavior with different eccentricities and under the influence of both conservative and non-conservative perturbing forces. Since the position error is always referred to a given epoch and, moreover, the physical time is not the independent variable, the accuracy in time will in general affect the computation of position even in the presence of only time-independent perturbations.

We propose five benchmark problems to be used as examples; these are taken from the paper Baù et al. (2013) and for easy reference are labeled by the letter E followed by a number from 1 to 5 as can be seen in Table 1. The initial position and velocity are specified as follows. Let the basic rectangular frame (O, x_1, x_2, x_3) have the origin O in Earth's barycenter and fixed directions in space, with the axes x_1 and x_2 lying on the equatorial plane and x_3 pointing to the North Pole. The object is located with respect to this frame in:

$$r_1 = 0\,\mathrm{km}, \qquad r_2 = -5888.9727\,\mathrm{km}, \qquad r_3 = -3400\,\mathrm{km},$$

Table 1
Examples Considered for the Numerical Tests

Example	Eccentricity	Perturbation
E1	0.95[a]	J_2
E2	0	J_2 + drag
E3	0.3	J_2 + Moon
E4	0.7	J_2 + Moon
E5	0.95[a]	J_2 + Moon

Note. [a] The value is not exactly equal to 0.95 as explained in the text.

which is the position shown in Table 1 of Baù et al. (2013). Assume the velocity is oriented along the positive x_1 axis and the propagated body is at the perigee. Therefore, for the velocity vector we have:

$$v_1 = v_c\sqrt{1+e_0}, \qquad v_2 = 0, \qquad v_3 = 0,$$

where v_c is the velocity of a circular orbit with radius equal to the initial orbital distance and e_0 is the initial eccentricity. The second column of Table 1 shows the value of e_0 of each example. For E1 and E5 v_1 is set equal to $10.691338\,\mathrm{km\,s^{-1}}$ as reported in Table 1 of Baù et al. (2013), which gives rise to an eccentricity almost equal to 0.95. Note that for the case of near-circular orbits, ordinary integration of position and velocity in the physical time would already be quite efficient. However, the use of a time transformation (and regularization in general) can still bring a further improvement in performance. This comes from the fact, as pointed out by Baumgarte (1972) and Velez (1974), that Equation (1) can reduce and even remove the dynamical instability of the Newtonian equations written for circular Keplerian motion.

The third column of Table 1 contains the applied perturbations, which are represented by the second zonal harmonic of the geopotential (J_2), the gravitational attraction of the Moon, and the atmospheric drag. The formulae implemented to compute the corresponding perturbing forces and the values of the physical constants therein are found in the section titled "Performance of the method" in Baù et al. (2013). It is worth pointing out that the lunar attraction depends explicitly on the physical time through the Moon's position and that it is not derived from a disturbing potential but regarded as a $\boldsymbol{P}$-type force (Equation (2)). On the other hand, the potential energy associated with the J_2 term is introduced.

The formulations compared in the numerical tests are listed in Table 2. Dromo is the method presented in Peláez et al. (2007); Dromo(P) is the improved version of Dromo for taking advantage of forces that are derived from disturbing potentials (Baù et al. 2013); the Dromo(PL) and Dromo(PC) schemes are based on the seven generalized orbital elements of Dromo(P) supplied by, respectively, the linear and constant time elements, ζ_0 and τ_0, developed in this paper. The Dromo(P) schemes are implemented with the total energy ε in place of ζ_3 (Equation (19)) as the dependent variable. We also include two other formulations known to be efficient in the orbit computation: the Sperling–Burdet (Spe&Bu) variables as described in Chapter 9 of the book Bond & Allman (1996) and the Stiefel–Scheifele (Sti&Sche) set of elements as implemented in Section 19 of the book Stiefel & Scheifele (1971). As highlighted in Table 2, Spe&Bu and Sti&Sche are characterized by a time transformation with an exponent of 1 instead of 2 and they describe the motion with two and six more dependent variables than the family of Dromo methods. Finally, we stress that in this paper, both methods are implemented with the use of a time element variable, while in Baù et al. (2013), the physical time was employed instead.

Table 2
Methods to be Compared

Method	Time Transformation	Dim.[a]	Time	Time el.
Dromo	$h\,\mathrm{d}t = r^2\,\mathrm{d}s$	8	x	
Dromo(P)	$c\,\mathrm{d}t = r^2\,\mathrm{d}s$	8	x	
Dromo(PL)	$c\,\mathrm{d}t = r^2\,\mathrm{d}s$	8		x
Dromo(PC)	$c\,\mathrm{d}t = r^2\,\mathrm{d}s$	8		x
Spe&Bu	$\mathrm{d}t = r\,\mathrm{d}s$	14		x
Sti&Sche	$\sqrt{-2\varepsilon}\,\mathrm{d}t = r\,\mathrm{d}s$	10		x

Notes. Apart from Dromo and Dromo(P), the other formulations employ a time element. The time transformation is the same for Dromo(P), Dromo(PL), and Dromo(PC). The fictitious time is indicated by s and the physical time by t. The quantities r, h, c, and ε are, respectively, the orbital radius, the osculating angular momentum, the generalized angular momentum (Equation (4)), and the total energy.
[a] This is the number of dependent variables.

3.2. Computational Cost versus Accuracy

Since the performance/price ratio of modern processor units is becoming increasingly high, the selection of an orbit propagator should be mainly guided by the accuracy requirement and secondly by the computational effort. Nonetheless, for intensive tasks, such as the orbit propagation of thousands of objects (i.e., asteroids and space debris) and the study of the evolution of natural bodies (i.e., the planets of the solar system) over long-time scales, even relatively small time savings in the propagation of each individual orbit would be significant. Therefore, we assess the efficiency of the methods in Table 2 by taking into account the computational cost spent to achieve a certain level of accuracy.

The first test consists of evaluating the error in the position at a target time t_f elapsed from the initial time 0. The adopted numerical integrator is the Runge–Kutta (4, 5) pair of Dormand & Prince (1980), hereafter called DP54, as implemented in the function ode45.m of the Matlab system. The step size is controlled by the algorithm itself by means of an absolute and relative tolerance. The first is set equal to 10^{-13} while the latter is allowed to take decreasing values in the range from 10^{-6} to 10^{-10}. For a given benchmark problem (Table 1), formulation (Table 2), and relative tolerance of the integrator DP54, the propagation is stopped when the physical time equals the time t_f. The computational cost is measured by the total number of evaluations on the right-hand side of the differential equations of motion, that is, the *function calls*. The position error is given by $|\boldsymbol{r}_f - \boldsymbol{r}_{ref}|$ where $\boldsymbol{r}_f$ is the position at time t_f computed at the end of the propagation and $\boldsymbol{r}_{ref}$ is the reference position, which represents the "exact" point where the object is at time t_f. It is expected that as the relative tolerance takes smaller values, the number of function calls increases and position error decreases as shown in Figures 2 and 4–7 for the five examples of Table 1. The time span of propagation t_f is specified in mean solar days (msd) in the caption of each figure along with the corresponding number of revolutions (revs) and the reference positions can be found in Table 2 of Baù et al. (2013). The delicate aspects concerning the selection of t_f for each example, the procedure applied to stop propagations at t_f, and the method for finding the reference positions are addressed in Baù et al. (2013).

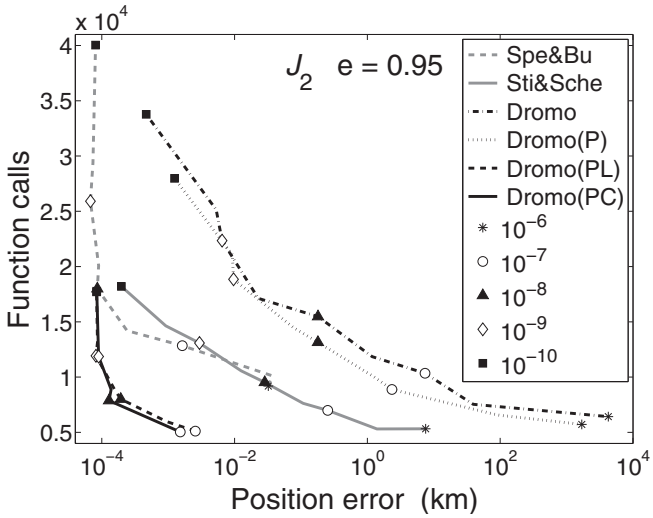

Figure 2. Function calls vs. position error for the example E1. Markers indicate different values of the relative tolerance of the fifth-order explicit Runge–Kutta method (DP54). The time span of propagation is 289.66457509 msd (50.5 revs). The curves of Dromo(PL) and Dromo(PC) almost overlap.

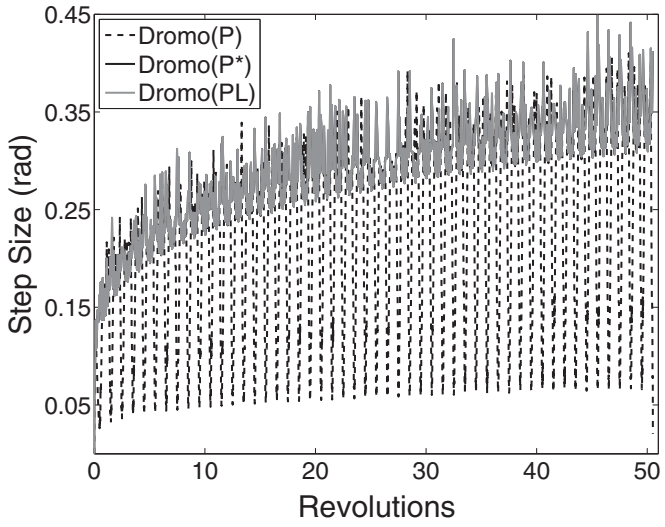

Figure 3. Step size variation for the example E1 with the relative tolerance of the fifth-order explicit Runge–Kutta method (DP54) set equal to 10^{-8}. In Dromo(P*), the time transformation (Equation (3)) is not numerically integrated. The introduction of a linear time element does not produce any appreciable variation of the step size with respect to Dromo(P*).

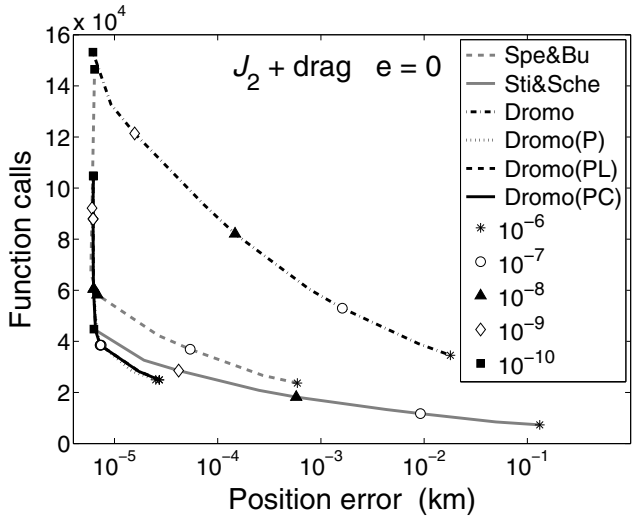

Figure 4. Same as Figure 2 but for the example E2. The numerical integrator is the fifth-order explicit Runge–Kutta method (DP54) and the time span of propagation is 9.68198362 msd (150 revs). The curves of Dromo(P), Dromo(PL), and Dromo(PC) almost overlap.

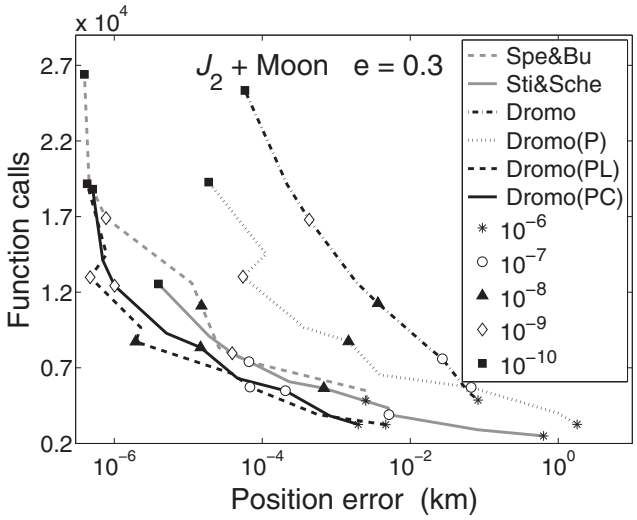

Figure 5. Same as Figure 2 but for the example E3. The numerical integrator is the fifth-order explicit Runge–Kutta method (DP54) and the time span of propagation is 5.45405849 msd (49.5 revs).

In the example E1 (Figure 2), the proposed time elements significantly improve the performance of Dromo(P) by requiring much lower function evaluations to reach better accuracies. In Figure 3, we plot the variation of the step length during the propagation for Dromo(P), Dromo(PL), and Dromo(P*), which refers to the Dromo(P) method without integrating the differential equation of the physical time. It is seen that in Dromo(P), the change of the step size is mainly controlled by the physical time and that Dromo(PL) produces the same curve as Dromo(P*), thus explaining why the time element poses such a huge benefit. The same effect was also noted by Ferrándiz et al. (1992a) for the set of *focal* coordinates and it motivated the introduction of a time element to be used with these variables (Ferrándiz & Sansaturio 1990). It is remarkable that Dromo(PL) and Dromo(PC) are, by far, superior to the other formulations in the main satellite problem for highly eccentric orbits.

Because the motion is nearly circular in the example E2 (Figure 4), the physical time behaves like a *linear* time element, and as expected, Dromo(PL) and Dromo(PC) are comparable to Dromo(P), which, by the way, already shows the best performance.

In the examples E3 (Figure 5), E4 (Figure 6), and E5 (Figure 7), it is seen that, as the initial eccentricity becomes higher and thereby the Moon's attraction stronger near the apogee, the benefit generated by the time elements with respect to the integration of the physical time is reduced. However, in E3 and E4, Dromo(PL) and Dromo(PC) outperform the other methods, while in E5, even if Sti&Sche ranks first, Dromo(PC) achieves up to two orders of magnitude better accuracies than Dromo(P) for the same range of function evaluations.

Note that the constant time element τ_0 is worse than the linear time element ζ_0 only in the example E3, showing in the other cases either a comparable or better behavior.

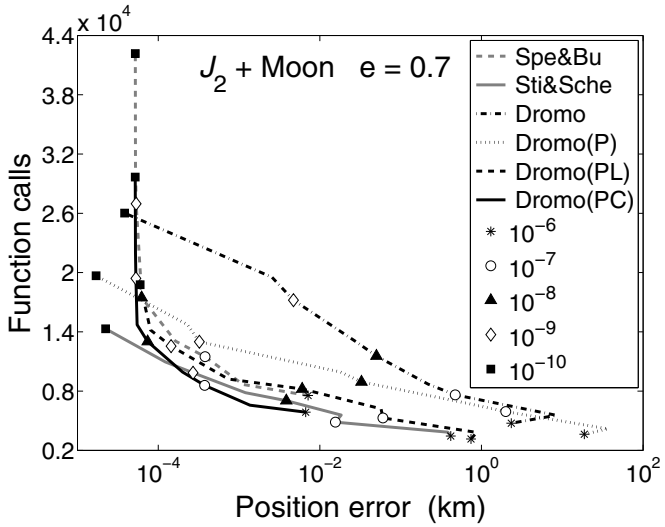

Figure 6. Same as Figure 2 for the example E4. The numerical integrator is the fifth-order explicit Runge–Kutta method (DP54) and the time span of propagation is 19.43348169 msd (49.5 revs).

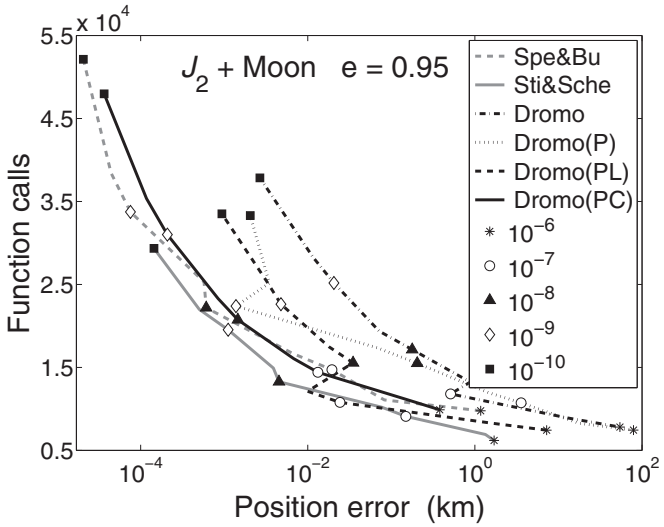

Figure 7. Same as Figure 2 for the example E5. The numerical integrator is the fifth-order explicit Runge–Kutta method (DP54) and the time span of propagation is 288.12768941 msd (49.5 revs).

One final remark concerns the computational time. The substitution of the physical time with a time element in the Dromo(P) method introduces additional mathematical operations with consequently little increase in the computational time spent per each integration step. In the example E2, the proposed time elements do not have any advantage with respect to Dromo(P). Therefore, we expect Dromo(P) will be slightly faster than Dromo(PL) and Dromo(PC). On the other hand, in the remaining examples, the difference in the function calls can be significant, in which case the new formulations run much faster than Dromo(P).

3.3. Error Growth

Another important performance metric is represented by the error growth in the position and time throughout the propagation. Several ways of estimating the global accuracy of numerical integrations exist when the exact solution is unknown (Fukushima 2003). The one adopted here consists of carrying out two integrations and taking the difference between them. For the examples E1–E4, we select the eighth-order implicit Adams method (AM8) in PECE mode (predict, evaluate, correct, evaluate) whose starting values are provided by a fifth-stage implicit Runge–Kutta algorithm. In the first propagation, the step size is given by $h = s_P/N$, where s_P is the value of the independent variable of the formulation to be tested corresponding to one period of the initial osculating orbit and N is the number of steps per revolution. In the second propagation, which is assumed to provide the *reference* solution, the step length is halved. Both the integrations are stopped when the particle would complete 5000 revolutions if the motion were unperturbed. The error in the position $\boldsymbol{r}$ at a certain physical time is assessed by means of the first-order Taylor expansion (Fukushima 2007):

$$\delta_r = \left| \boldsymbol{r}_h - \boldsymbol{r}_{h/2} - \delta_t \, \boldsymbol{v}_{h/2} \right|, \tag{42}$$

where the subscripts refer to the step size of the integration, $\boldsymbol{v}$ is the velocity vector, and δ_t is the error of the physical time:

$$\delta_t = |t_h - t_{h/2}|. \tag{43}$$

In Figures 8–11, the position and time errors δ_r and δ_t relative to the examples E1–E4 of Table 1 are displayed as a function of the normalized coordinate:

$$\chi = s/\max(s), \tag{44}$$

where s represents the independent variable of each formulation (as shown in the second column of Table 2). The value of N, which is reported in each figure, has been chosen in order to avoid both the numerical instability and the dominance of the round-off error.

In the example E5, a fixed step size integrator is not appropriate for a time transformation with the exponent α in Equation (1) equal to 2 while it is still a good choice when α is equal to 1. The reason is that for the same N the analytic step size regulation produced by $\alpha = 1$ places more points near the apogee where the Moon exerts a stronger attraction (which is significantly higher than in E4[5]). Indeed, if the same integrators selected for E1–E4 are adopted in E5 and N is set equal to 144 one finds that after 5000 revs Sti&Sche is five orders of magnitude more accurate in the position than all Dromo methods (which show almost the same performance). This huge difference is mainly due to the quadratic error growth of the formers against the linear increase of the latter. Thus, we prefer to use the numerical integrator DP54 already employed in the tests from the previous section. We stress that while the variable step size seems to be necessary for the Dromo formulations, there should not be much benefit to having it with methods relying on a Sundman time transformation of order 1 (such as Spe&Bu and Sti&Sche).

In this case, two integrations are conducted with different relative tolerances: 10^{-7} is selected for the *test* propagation and 10^{-9} to obtain the *reference* solution. The reference position and time are provided at the required values of the independent variable by interpolation through the Matlab function ntrp45.m. Finally, the errors are computed with formulae analogous to Equations (42) and (43) and are shown in Figure 12 over 5000 "unperturbed" revolutions.

[5] For example, the maximum value of the ratio between the forces due to the Moon and Earth is three orders of magnitude bigger in E5 than in E4.

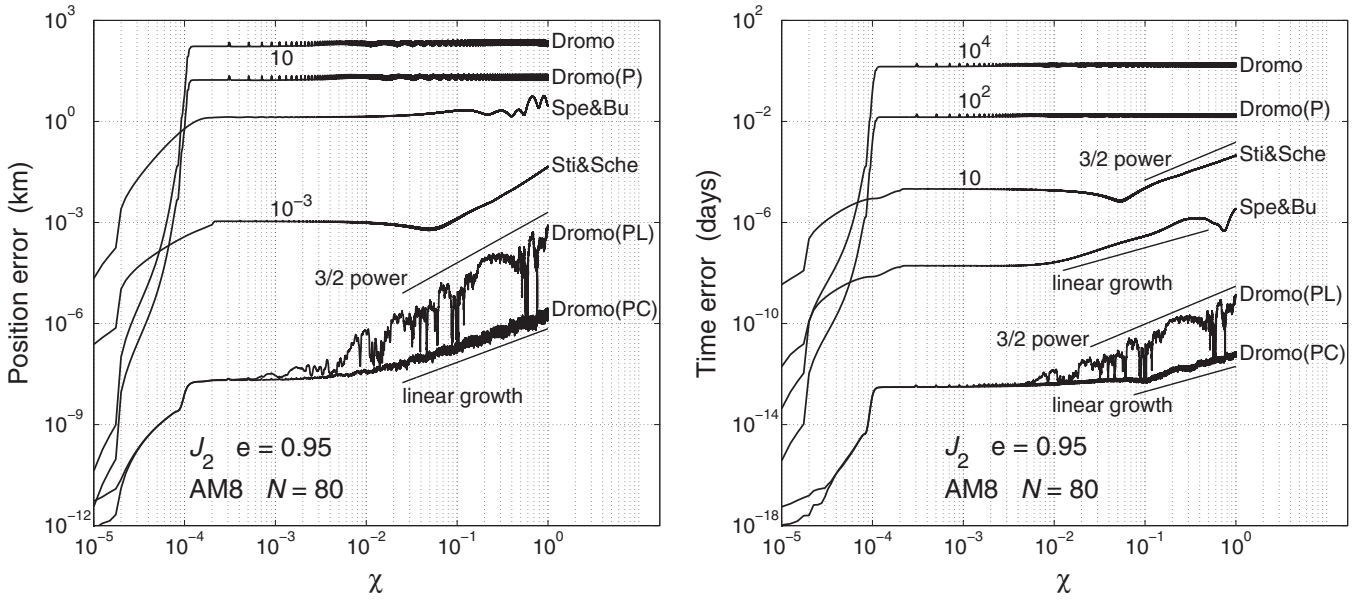

Figure 8. Position error (Equation (42)), left, and time error (Equation (43)), right, as a function of χ (Equation (44)) in the example E1 for 5000 revs. The numerical integrator is the eighth-order Adams in PECE mode (AM8) and N is the number of steps per rev.

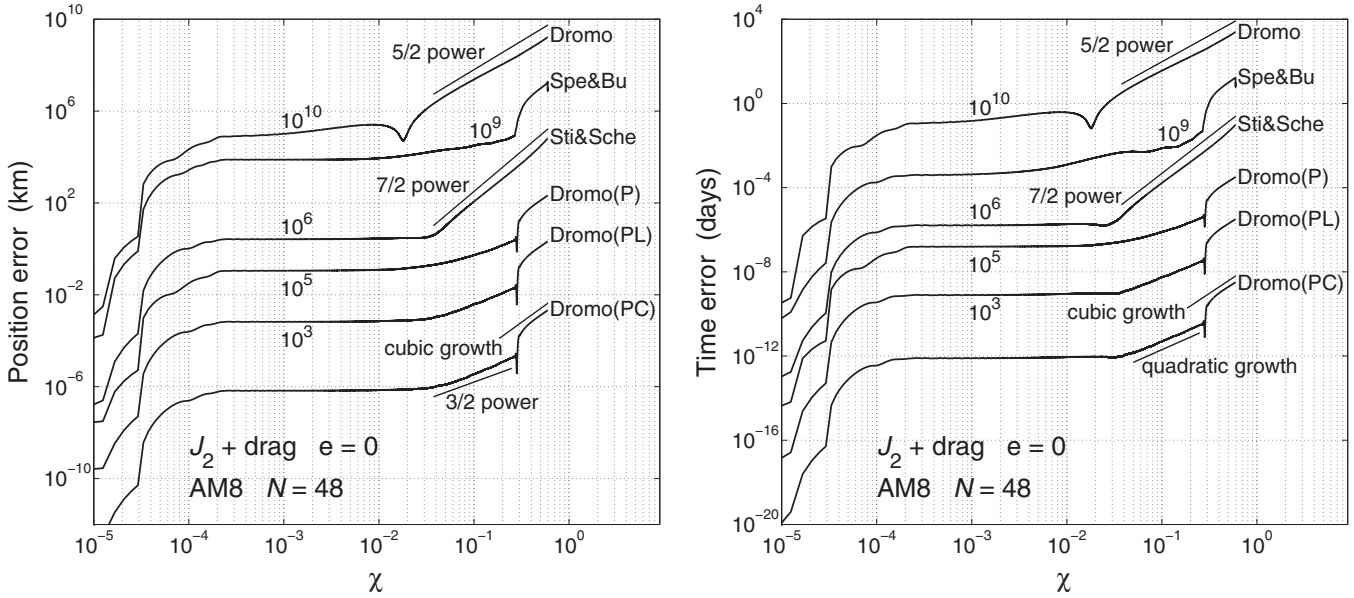

Figure 9. Position error (Equation (42)), left, and time error (Equation (43)), right, as a function of χ (Equation (44)) in the example E2 for 5000 revs. The numerical integrator is the eighth-order Adams in PECE mode (AM8) and N is the number of steps per rev. The error is shown up to 2980 revs, just before which a big jump in the error is observed (this kind of instability cannot be eliminated by changing the value of N in the AM8 or the numerical integrator).

The performance diagrams show average errors that are obtained by a moving average filter.[6] Besides, in order to avoid superpositions, the curves are shifted along the vertical axis when necessary by a suitable power of 10.

In the example E1 (Figure 8), the proposed time element τ_0 to be used in combination with the spatial variables of Dromo(P) drastically reduces the position and time errors with respect to the direct integration of the physical time. Although Dromo(PC) exhibits a linear increase of the error compared to the constant behavior observed in Dromo(P) (and Dromo), it is seven orders of magnitude more accurate in the position at the end of the propagation. We note that the error grows linearly for Dromo(PC) and Spe&Bu which employ a *constant* time element, while it becomes proportional to the 3/2 power of the independent variable when a *linear* time element is adopted, as in Dromo(PL) and in Sti&Sche, which is the typical law of the round-off error (Brouwer 1937). The reason for this is that since the orbit is highly eccentric and the J_2 perturbation weakens as the propagated body goes away from the Earth, for most of the integration, the time element is given by the sum of an increasingly big term proportional to the independent variable and a small perturbing quantity (see Equation (33)).

The introduction of a time element does not essentially change the error evolution of Dromo(P) in E2 (Figure 9), and it further improves the already good performance of the method so that

[6] More precisely, the window size exploits $m + 1$ points where we have set m equal to the number of steps per revolution (N) for the examples E1–E4, and to 5 floor $(n/5000)$ for E5, with n being the number of steps of the whole integration.

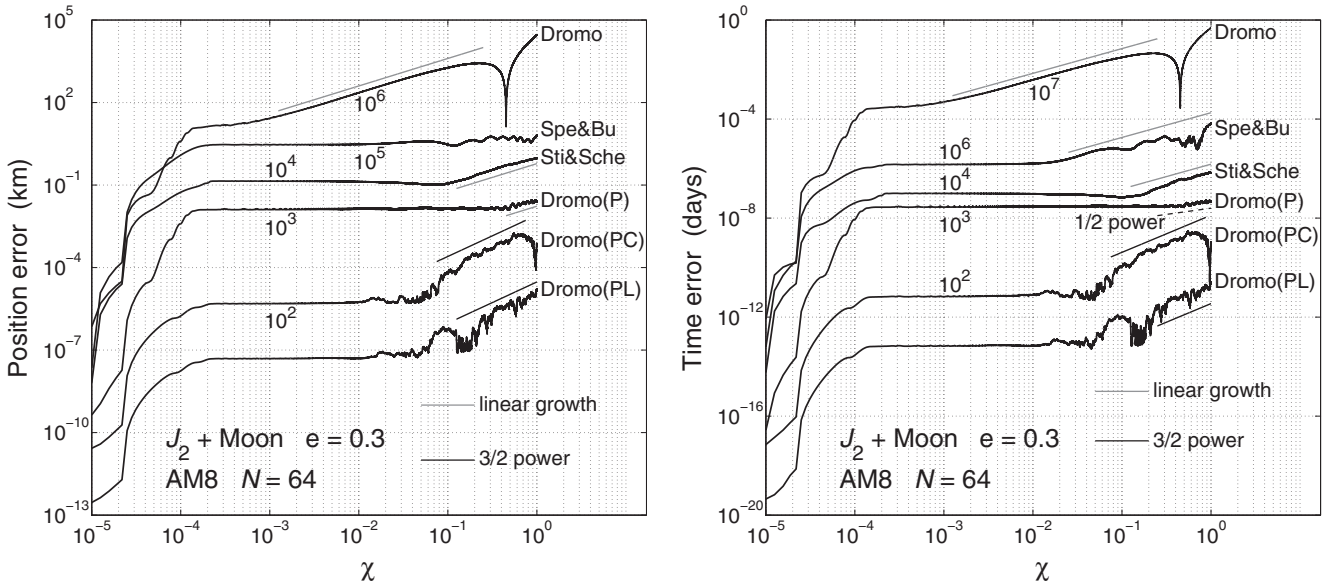

Figure 10. Position error (Equation (42)), left, and time error (Equation (43)), right, as a function of χ (Equation (44)) in the example E3 for 5000 revs. The numerical integrator is the eighth-order Adams in PECE mode (AM8) and N is the number of steps per rev.

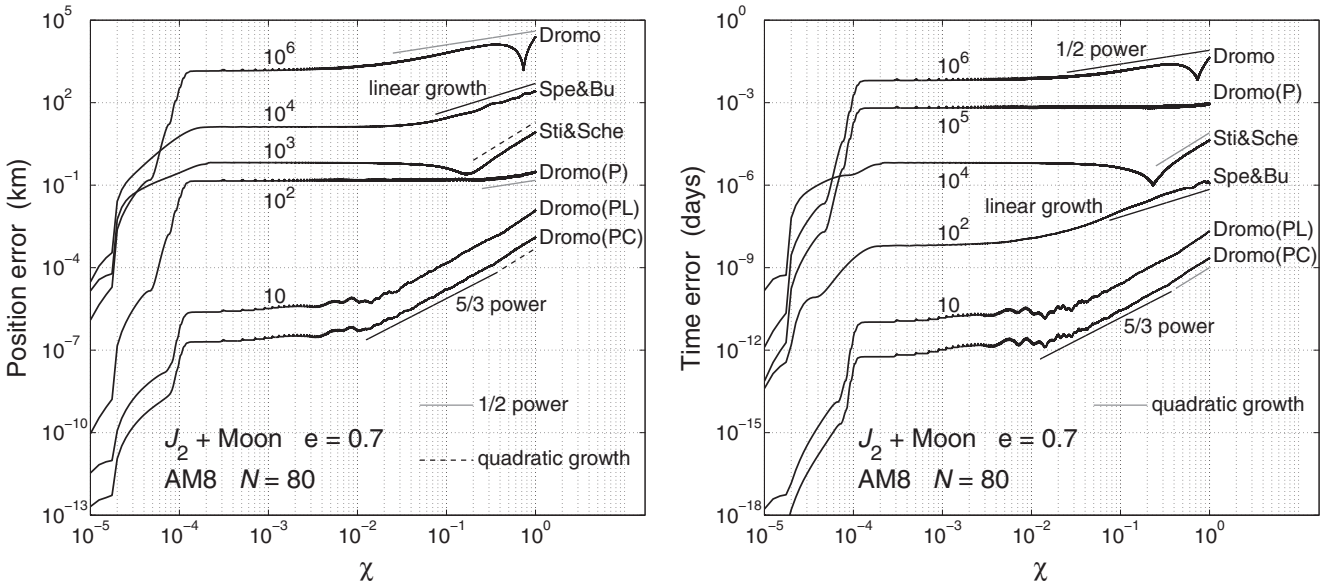

Figure 11. Position error (Equation (42)), left, and time error (Equation (43)), right, as a function of χ (Equation (44)) in the example E4 for 5000 revs. The numerical integrator is the eighth-order Adams in PECE mode (AM8) and N is the number of steps per rev.

out of the compared formulations, Dromo(PC) and Dromo(PL) generate the smallest position error throughout the propagation. After an initial plateau, the error increases roughly obeying to the power $3/2$ (position) and 2 (time) up to around 1350 revolutions when a jump occurs, then the growth becomes cubic. An analogous jump is also found in Spe&Bu after which the error increases according to a $7/2$ power law. This scheme is the most accurate in the computation of time during the first 35 revolutions followed by Dromo(PC) and Dromo(PL) which, thereafter, are the best. In Dromo and Sti&Sche, the position and time errors start growing quite early, at around 100 and 150 revolutions, with a $5/2$ and $7/2$ index power, respectively.

Let us analyze the performance when the gravitational attraction of the Moon is considered along with the J_2 perturbation. The time elements τ_0 and ζ_0 reduce the initial error amplification of Dromo(P) by more than two and three orders of magnitude, respectively, in the examples E3 (Figure 10) and E4 (Figure 11). After remaining constant, the errors increase at around 250 revs in E3 and 50 revs in E4 as the $3/2$ (E3) and $5/3$ - 2 (E4) powers of the independent variable compared to the at most linear accumulation shown by Dromo(P) and the other formulations (with Sti&Sche, which is affected by a quadratic growth in E4, being the only exception). Nonetheless, Dromo(PC) and Dromo(PL) generate again the smallest averaged errors which become comparable to those of Dromo(P) at the end of the propagation. In E5 (Figure 12), the constant time element τ_0 does not alter the $3/2$ power growth of the error in Dromo(P) while Dromo(PL), like Dromo and Sti&Sche, is characterized by a quadratic evolution. It is notable that, even with a higher relative tolerance (10^{-6} instead of 10^{-7}), Dromo(PC) shows the second best accuracy after Sti&Sche with a similar error in the last part of the propagation thanks to the smaller rate of change.

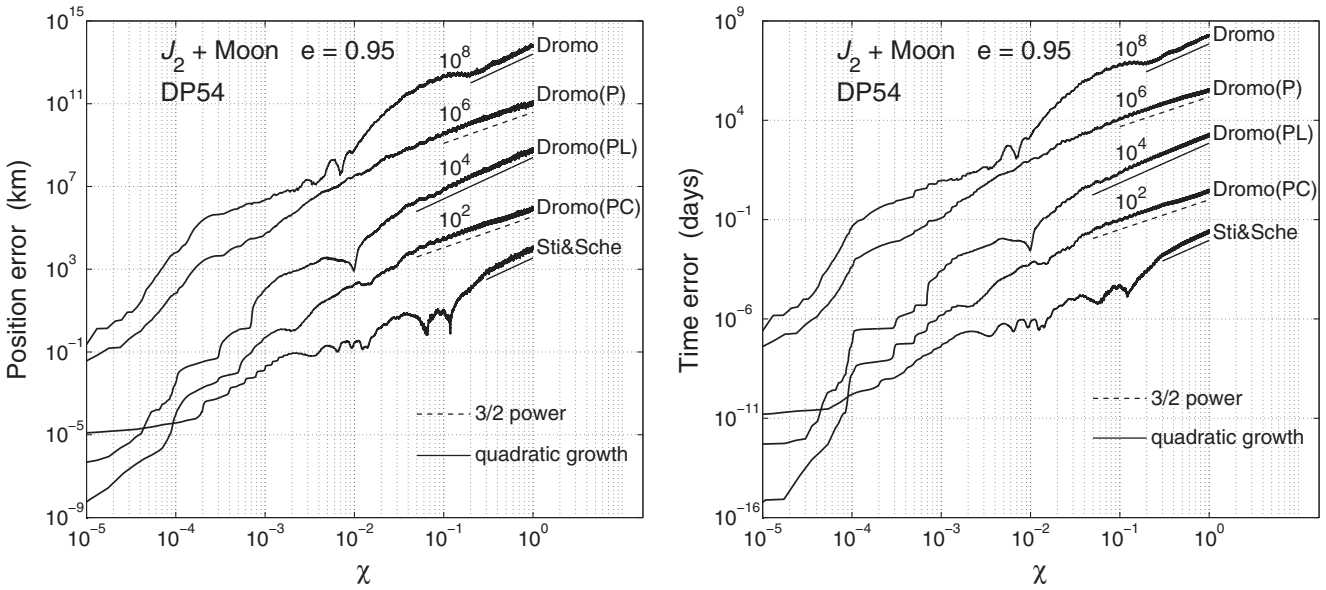

Figure 12. Position error (Equation (42)), left, and time error (Equation (43)), right, as a function of χ (Equation (44)) in the example E5 for 5000 revs. The numerical integrator is the fifth-order explicit Runge–Kutta method (DP54). The relative tolerance for obtaining the error is set equal to 10^{-6} for Dromo(PC) instead of 10^{-7} in order to render the number of integration steps comparable with that of the other methods. The Sperling–Burdet formulation is not shown since it exhibits a very poor performance.

Finally, we can state that Dromo(PL) (linear time element ζ_0) is better than Dromo(PC) (constant time element τ_0) in the presence of weak non-conservative perturbations and with moderate eccentricities (example E3). In the other examples, either the two methods are equivalent (E2 and E4) or Dromo(PC) outperforms Dromo(PL) (E1 and E5).

4. CONCLUSIONS

Two time elements have been developed to be used with spatial variables of the formulation of the perturbed two-body problem called Dromo(P), both of them leading to equations free of singularities and limitations due to the multi-value arctangent function. The theory has been presented for a negative total energy and the cases of zero and positive total energy are addressed in Appendix B.

One time element is a linear function of the independent variable; the other one is an integral of Keplerian motion. The resulting equations are also defined for circular motion, which instead represents a singularity in analogous time elements found in the literature. Moreover, the second proposed time element represents the first example of a constant time element associated with a time transformation with exponent 2 which does not present any limitation stemming from the multi-revolution issue.

The benefit introduced by the time elements is impressive in the main satellite problem, and in particular the formulation with the constant time element is by far the best formulation in terms of propagation accuracy versus function calls and reduction of the position as well as time errors with respect to the independent variable. When non-conservative perturbations are added (atmospheric drag, the Moon's gravitational attraction) to the J_2 zonal harmonic, either of the two proposed formulations keeps showing the smallest errors among the compared schemes up to high eccentricities. Concerning the error evolution, the proposed time elements compared with the direct employment of the physical time in Dromo(P) enjoys a significantly smaller initial error. However, after remaining constant, it undergoes an earlier and faster increase (which approaches the quadratic law as the eccentricity grows) so that after a sufficiently large number of revolutions (5000 in the examples), the errors become comparable. Therefore, we suggest switching to a Dromo formulation without time element for very long propagations since this method exhibits a more favorable behavior (at most, a linear growth of the error) as long as the magnitude of the non-conservative perturbations is moderate.

In general, the constant time element outperforms the linear one, the latter being preferable only in the example of moderately eccentric motion perturbed by Earth's oblateness and lunar attraction.

We thank M. E. Sansaturio for sending several relevant papers on the topic. Comments by the referee have been helpful in improving the quality of the paper.

APPENDIX A

TIME ELEMENT ζ_0

A.1. Implementation of the Time Element ζ_0 in the Dromo(P) Method

The new state vector of the Dromo(P) method is composed of eight elements ζ_i, $i = 0, \ldots, 7$. The initialization of the time element ζ_0 at time $t = 0$ from the position and velocity is done by exploiting Equation (32) where ζ_1, ζ_2, and ζ_3 are evaluated through Equations (7), (8), and (19). The numerical integration of Equation (33) produces the current value of ζ_0 which, in turn, is plugged into Equation (32) to get the physical time.

Besides, if the total energy ε is a dependent variable, then in Equations (32) and (33), the element ζ_3 is given by:

$$\zeta_3 = \sqrt{\zeta_1^2 + \zeta_2^2 - 2\,\varepsilon},$$

while if ζ_3 is a dependent variable, the total energy ε is obtained by:

$$\varepsilon = \frac{\zeta_1^2 + \zeta_2^2 - \zeta_3^2}{2}.$$

A.2. Expression for $G-\theta$ (Equation (26))

By exploiting the half-angle and angle difference identities for the trigonometric functions, we have:

$$\tan\left(\frac{G-\theta}{2}\right)=\frac{\sin G\cos\theta-\sin\theta\cos G}{1+\cos G\cos\theta+\sin G\sin\theta}.$$

For convenience, let us introduce the quantity:

$$\beta=\sqrt{1-g^2}+1.$$

Then, we plug in the expressions for $\sin G$ and $\cos G$ reported in Equation (21) to find:

$$\tan\left(\frac{G-\theta}{2}\right)=\frac{[(\beta-2)\,\cos\theta-g]\sin\theta}{2\,(1+g\,\cos\theta)+(\beta-2)\,\sin^2\theta}. \tag{A1}$$

By exploiting the identity:

$$(\beta-2)\,\beta=-g^2, \tag{A2}$$

we rewrite the numerator in Equation (A1) as:

$$[(\beta-2)\,\cos\theta-g]\sin\theta=-(1+g\,\beta^{-1}\,\cos\theta)\,g\,\sin\theta, \tag{A3}$$

and the denominator as:

$$2\,(1+g\,\cos\theta)+(\beta-2)\,\sin^2\theta=\beta^{-1}\,(\beta+g\,\cos\theta)^2\,. \tag{A4}$$

Equations (A3) and (A4) are used into Equation (A1) to give the final result:

$$\tan\left(\frac{G-\theta}{2}\right)=-\frac{g\sin\theta}{\beta+g\cos\theta},$$

from which Equation (26) is directly obtained.

A.3. Differential Equation of ζ_0 ($\varepsilon<0$, Equation (33))

Let us write the differential equation of ζ_3, which is Equation (35) on p. 63 of Baù et al. (2013), with the help of Equation (38) of this paper as:

$$\frac{\mathrm{d}\zeta_3}{\mathrm{d}\phi}=\frac{\zeta_3}{s^2}\left[\frac{u}{s}\left(\frac{R}{\zeta_3\,s}-2\,\mathcal{U}\right)-\frac{\mathrm{d}\varepsilon}{\mathrm{d}\phi}\right], \tag{A5}$$

where s and u are given in Equations (28) and (29). This expression is plugged into Equations (33) and (34) on p. 62 of Baù et al. (2013), which take the form:

$$\begin{aligned}\frac{\mathrm{d}\zeta_1}{\mathrm{d}\phi}=&\frac{1}{s^3}\left(\frac{R}{\zeta_3\,s}-2\,\mathcal{U}\right)\left[\zeta_2\,(\zeta_3+s)+\zeta_3^2\sin\phi\right]\\&+\frac{1}{s^2}\frac{\mathrm{d}\varepsilon}{\mathrm{d}\phi}\,(\zeta_3+s)\cos\phi,\end{aligned} \tag{A6}$$

$$\begin{aligned}\frac{\mathrm{d}\zeta_2}{\mathrm{d}\phi}=&-\frac{1}{s^3}\left(\frac{R}{\zeta_3\,s}-2\,\mathcal{U}\right)\left[\zeta_1\,(\zeta_3+s)+\zeta_3^2\cos\phi\right]\\&+\frac{1}{s^2}\frac{\mathrm{d}\varepsilon}{\mathrm{d}\phi}\,(\zeta_3+s)\sin\phi.\end{aligned} \tag{A7}$$

Proceed with the differentiation of Equation (32):

$$\frac{\mathrm{d}\zeta_0}{\mathrm{d}\phi}=\frac{\mathrm{d}t}{\mathrm{d}\phi}+\frac{\mathrm{d}}{\mathrm{d}\phi}\left(\frac{a\,u}{\zeta_3\,s}\right)+\frac{\mathrm{d}}{\mathrm{d}\phi}\left(2\,a^{3/2}\arctan\left(\frac{u}{f+w}\right)\right), \tag{A8}$$

inserting the quantities a, w, and f as introduced in Equations (35)–(37). Substitute for c and r in Equation (3) as shown, respectively, in Equation (19) and in the first relation in (27) to find Equation (32) on p. 62 of Baù et al. (2013), that is:

$$\frac{\mathrm{d}t}{\mathrm{d}\phi}=\frac{1}{\zeta_3\,s^2}. \tag{A9}$$

The other two terms in Equation (A8) produce the expressions:

$$\begin{aligned}\frac{\mathrm{d}}{\mathrm{d}\phi}\left(\frac{a\,u}{\zeta_3\,s}\right)=&\frac{a}{\zeta_3\,s}\left\{S\,\frac{\mathrm{d}\zeta_1}{\mathrm{d}\phi}-C\,\frac{\mathrm{d}\zeta_2}{\mathrm{d}\phi}+w\right.\\&-\frac{u}{s}\left[\frac{\mathrm{d}\zeta_3}{\mathrm{d}\phi}\left(1+\frac{s}{\zeta_3}\right)+C\,\frac{\mathrm{d}\zeta_1}{\mathrm{d}\phi}+S\,\frac{\mathrm{d}\zeta_2}{\mathrm{d}\phi}-u\right]\\&\left.+2\,a\,u\,\frac{\mathrm{d}\varepsilon}{\mathrm{d}\phi}\right\},\end{aligned} \tag{A10}$$

and:

$$\begin{aligned}\frac{\mathrm{d}}{\mathrm{d}\phi}\left(2\,a^{3/2}\arctan\left(\frac{u}{f+w}\right)\right)=&\,6\,a^{5/2}\,\frac{\mathrm{d}\varepsilon}{\mathrm{d}\phi}\arctan\left(\frac{u}{f+w}\right)\\&+\frac{a^{3/2}}{s\,f}\left[\left(S\,\frac{\mathrm{d}\zeta_1}{\mathrm{d}\phi}-C\,\frac{\mathrm{d}\zeta_2}{\mathrm{d}\phi}+w\right)(f-w)\right.\\&\left.-u\left(\frac{\mathrm{d}\zeta_3}{\mathrm{d}\phi}+C\,\frac{\mathrm{d}\zeta_1}{\mathrm{d}\phi}+S\,\frac{\mathrm{d}\zeta_2}{\mathrm{d}\phi}-\sqrt{a}\,\frac{\mathrm{d}\varepsilon}{\mathrm{d}\phi}-u\right)\right],\end{aligned} \tag{A11}$$

where $S=\sin\phi$ and $C=\cos\phi$. By inserting Equations (A5)–(A7) into Equations (A10) and (A11) and collecting similar terms, we have:

$$\frac{\mathrm{d}}{\mathrm{d}\phi}\left(\frac{a\,u}{\zeta_3\,s}\right)=\frac{a}{\zeta_3\,s}\left[w+\frac{u^2}{s}+\frac{1}{s}\left(\frac{R}{\zeta_3\,s}-2\,\mathcal{U}\right)+2\,a\,u\,\frac{\mathrm{d}\varepsilon}{\mathrm{d}\phi}\right], \tag{A12}$$

and:

$$\begin{aligned}&\frac{\mathrm{d}}{\mathrm{d}\phi}\left(2\,a^{3/2}\arctan\left(\frac{u}{f+w}\right)\right)\\&\quad=a^{3/2}-\frac{a}{s}+6\,a^{5/2}\,\frac{\mathrm{d}\varepsilon}{\mathrm{d}\phi}\arctan\left(\frac{u}{f+w}\right)\\&\qquad+\frac{a^{3/2}}{s^2\,f}\left[\left(\frac{R}{\zeta_3\,s}-2\,\mathcal{U}\right)\left(f+w+\frac{u^2}{s}\right)\right.\\&\qquad\left.+\frac{\mathrm{d}\varepsilon}{\mathrm{d}\phi}\,u(s\,\sqrt{a}-1)\right].\end{aligned} \tag{A13}$$

The sum of the right-hand sides of Equations (A9), (A12), and (A13) and use of the relation $u^2=2\,s\,\zeta_3-s^2+2\,\varepsilon$ yield the differential Equation (33).

APPENDIX B

TIME ELEMENTS FOR POSITIVE AND ZERO VALUES OF THE TOTAL ENERGY

Let us assume that the total energy is positive. Integration of the time transformation (3) in the unperturbed motion with r taken from Equation (20) gives the generalized Kepler's equation for $\varepsilon>0$:

$$\begin{aligned}t=\tau_p+&\frac{c\,g\,\sin\theta}{2\,\varepsilon(1+g\,\cos\theta)}\\&-\frac{2}{(2\,\varepsilon)^{3/2}}\operatorname{arctanh}\left(\frac{\sin\theta}{1+\cos\theta}\sqrt{\frac{g-1}{g+1}}\right),\end{aligned}$$

where from Equation (5) we have that $g > 1$. By using the relations (19) and (30), the above equation is brought into the form:

$$t = \tau_p + \frac{u\,a}{\zeta_3\,s} - 2\,a^{3/2}\,\mathrm{arctanh}\left(\frac{u}{\zeta_3\,g + w}\sqrt{\frac{g-1}{g+1}}\right), \quad \text{(B1)}$$

where w is reported in Equation (36) and $a = 1/(2\,\varepsilon)$. In contrast to the case $\varepsilon < 0$, the constant of integration τ_p can be chosen as a time element. In order to exploit Equation (B1) for computing the physical time, the time element τ_p is required. In the two-body problem, τ_p is determined by the initial conditions and is a constant. In presence of perturbations, τ_p is obtained by the numerical integration of a first-order differential equation. To derive it, we differentiate Equation (B1):

$$\frac{\mathrm{d}\tau_p}{\mathrm{d}\phi} = \frac{\mathrm{d}t}{\mathrm{d}\phi} - \frac{\mathrm{d}}{\mathrm{d}\phi}\left(\frac{a\,u}{\zeta_3\,s}\right) + \frac{\mathrm{d}}{\mathrm{d}\phi}\left(2\,a^{3/2}\,\mathrm{arctanh}\left(\frac{u}{\zeta_3\,g + w}\sqrt{\frac{g-1}{g+1}}\right)\right). \quad \text{(B2)}$$

Taking advantage of Equation (A12) we carry out the derivatives:

$$\frac{\mathrm{d}}{\mathrm{d}\phi}\left(-\frac{a\,u}{\zeta_3\,s}\right) = -\frac{a}{\zeta_3\,s}\left[w + \frac{u^2}{s} + \frac{1}{s}\left(\frac{R}{\zeta_3\,s} - 2\,\mathcal{U}\right) - 2\,a\,u\,\frac{\mathrm{d}\varepsilon}{\mathrm{d}\phi}\right], \quad \text{(B3)}$$

and:

$$\begin{aligned}\frac{\mathrm{d}}{\mathrm{d}\phi}&\left(2\,a^{3/2}\,\mathrm{arctanh}\left(\frac{u}{\zeta_3\,g + w}\sqrt{\frac{g-1}{g+1}}\right)\right)\\ &= -6\,a^{5/2}\,\frac{\mathrm{d}\varepsilon}{\mathrm{d}\phi}\,\mathrm{arctanh}\left(\frac{u}{\zeta_3\,g + w}\sqrt{\frac{g-1}{g+1}}\right) + \frac{a^{3/2}\sqrt{g^2-1}}{s\,g}\\ &\quad\times\left[S\,\frac{\mathrm{d}\zeta_1}{\mathrm{d}\phi} - C\,\frac{\mathrm{d}\zeta_2}{\mathrm{d}\phi} + w - \frac{u}{\zeta_3\,g + w}\right.\\ &\quad\times\left.\left(\frac{\mathrm{d}(g\,\zeta_3)}{\mathrm{d}\phi} + C\,\frac{\mathrm{d}\zeta_1}{\mathrm{d}\phi} + S\,\frac{\mathrm{d}\zeta_2}{\mathrm{d}\phi} - u\right) + \frac{u}{g^2-1}\,\frac{\mathrm{d}g}{\mathrm{d}\phi}\right],\end{aligned}$$

where $S = \sin\phi$, $C = \cos\phi$ and we made use of the identity $u^2 + w^2 = \zeta_3^2\,g^2$. First, Equation (5) is exploited to substitute for $g^2 - 1$ and to find $\mathrm{d}g/\mathrm{d}\phi$, then Equations (A5)–(A7) are employed to get:

$$\begin{aligned}\frac{\mathrm{d}}{\mathrm{d}\phi}&\left(2\,a^{3/2}\,\mathrm{arctanh}\left(\frac{u}{\zeta_3\,g + w}\sqrt{\frac{g-1}{g+1}}\right)\right)\\ &= -6\,a^{5/2}\,\frac{\mathrm{d}\varepsilon}{\mathrm{d}\phi}\,\mathrm{arctanh}\left(\frac{u}{\zeta_3\,g + w}\sqrt{\frac{g-1}{g+1}}\right) + \frac{a}{\zeta_3\,s^3\,g^2}\\ &\quad\times\left[\left(\frac{R}{\zeta_3\,s} - 2\,\mathcal{U}\right)\left(\zeta_3\,g^2 + w\right) + \frac{\mathrm{d}\varepsilon}{\mathrm{d}\phi}\,u\,s\,\left(a\,s - \frac{1}{\zeta_3}\right)\right].\end{aligned} \quad \text{(B4)}$$

The expressions contained in Equations (A9), (B3), and (B4) are inserted into Equation (B2) and after some simplifications, the final result is:

$$\begin{aligned}\frac{\mathrm{d}\tau_p}{\mathrm{d}\phi} = &-6\,a^{5/2}\,\frac{\mathrm{d}\varepsilon}{\mathrm{d}\phi}\,\mathrm{arctanh}\left(\frac{u}{\zeta_3\,g + w}\sqrt{\frac{g-1}{g+1}}\right)\\ &+ \frac{r}{g^2}\left[\frac{\mathrm{d}\varepsilon}{\mathrm{d}\phi}\,a\,u\,\left(3\,a - r + \frac{2}{\zeta_3^2}\right) - (R\,r - 2\,\mathcal{U})\,w\,r^2\right],\end{aligned} \quad \text{(B5)}$$

where $r = 1/(\zeta_3\,s)$.

If the energy undergoes a change of sign during the numerical propagation, then one possible robust strategy for dealing with this case is to switch from the use of a time element to the physical time in the state vector whenever the magnitude of the total energy becomes sufficiently small.

For completeness, let us assume that the total energy is zero, which implies that $g = 1$. The generalized Barker's equation takes the form:

$$t = \tau_{p,1} + \frac{1}{6\,\zeta_3^3}\left(3\,\tan\frac{\theta}{2} + \tan^3\frac{\theta}{2}\right), \quad \text{(B6)}$$

which can be transformed into:

$$t = \tau_{p,1} + \frac{u\,r^2}{3}\left(\frac{s}{\zeta_3} + 1\right),$$

and the derivative of $\tau_{p,1}$ becomes:

$$\frac{\mathrm{d}\tau_{p,1}}{\mathrm{d}\phi} = \frac{r^3}{3}\left[(R\,r - 2\,\mathcal{U})\,3\,w + \frac{\mathrm{d}\varepsilon}{\mathrm{d}\phi}\,2\,u\right]. \quad \text{(B7)}$$

Equations (B1), (B5), and Equations (B6), (B7) are necessary to introduce a time element in the Dromo(P) method for the cases $\varepsilon > 0$ and $\varepsilon = 0$, respectively.

REFERENCES

Arakida, H., & Fukushima, T. 2001, AJ, 121, 1764
Baù, G., Bombardelli, C., & Peláez, J. 2013, CeMDA, 116, 53
Baumgarte, J. 1972, CeMec, 5, 490
Baumgarte, J. 1976, CeMec, 14, 121
Baumgarte, J., & Stiefel, E. 1974, in Lecture Notes in Mathematics, Vol. 362, Proc. Conf. Numerical Solution of Ordinary Differential Equations, ed. D. G. Bettis (Berlin: Springer), 207
Bombardelli, C., & Baù, G. 2012, CeMDA, 114, 279
Bombardelli, C., Baù, G., & Peláez, J. 2011, CeMDA, 110, 239
Bond, V. R. 1974, CeMec, 10, 303
Bond, V. R. 1982, CeMec, 27, 65
Bond, V. R., & Allman, M. C. 1996, Modern Astrodynamics: Fundamentals and Perturbation Methods (Princeton, NJ: Princeton Univ. Press)
Broucke, R. A., & Cefola, P. 1973, CeMec, 7, 388
Brouwer, D. 1937, AJ, 46, 149
Burdet, C. A. 1968, ZaMPh, 19, 345
Burdet, C. A. 1969, J. Reine Angew. Math., 238, 71
Deprit, A. 1975, JRNBS, 79B, 1
Dormand, J. R., & Prince, P. J. 1980, JCoAM, 6, 19
Feagin, T., & Mikkilineni, R. P. 1976, CeMec, 13, 491
Ferrándiz, J. M. 1988, CeMec, 41, 343
Ferrándiz, J. M., & Sansaturio, M. E. 1990, in XIV Jornadas Hispano-Lusas de Matemáticas, Vol. III, ed. N. H. Calil (La Laguna, Canary Islands: La Laguna Univ.), 1231
Ferrándiz, J. M., & Sansaturio, M. E. 1995, in From Newton to Chaos, ed. A. E. Roy & B. A. Steves, Vol. 336 (New York: Plenum), 545
Ferrándiz, J. M., Sansaturio, M. E., & Pojman, J. R. 1992a, CeMDA, 53, 347
Ferrándiz, J. M., Sansaturio, M. E., & Vigo, J. 1991, in Predictability, Stability, and Chaos in N-Body Dynamical Systems, ed. A. E. Roy, Vol. 272 (New York: Plenum), 387

Ferrándiz, J. M., Sansaturio, M. E., & Vigo, J. 1992b, in Proc. AAS/AIAA Spaceflight Mechanics Meeting, ed. R. E. Diehl et al. (San Diego, CA: Univelt), 1185
Ferrándiz, J. M., Sansaturio, M. E., & Vigo, J. 1993, in Instability, Chaos and Predictability in Celestial Mechanics and Stellar Dynamics, ed. K. B. Bhatnagar (Commack, NY: Nova Science Publishers), 353
Fukushima, T. 2003, AJ, 128, 1097
Fukushima, T. 2005, AJ, 129, 1746
Fukushima, T. 2007, AJ, 133, 2815
Janin, G. 1974, CeMec, 10, 451
Kwok, J. H., & Nacozy, P. 1981, CeMec, 24, 269
Levi-Civita, T. 1906, AcMA, 30, 305
Nacozy, P. 1976a, CeMec, 13, 495
Nacozy, P. 1976b, CeMec, 14, 129
Nacozy, P. 1981, CeMec, 23, 173
Peláez, J., Hedo, J. M., & de Andréz, P. R. 2007, CeMDA, 97, 131
Siegel, C. L., & Moser, J. K. 1971, Lectures on Celestial Mechanics, Classics in Mathematics (Berlin: Springer)
Stiefel, E. L., & Scheifele, G. 1971, Linear and Regular Celestial Mechanics (Berlin: Springer)
Sundman, K. F. 1912, AcMA, 36, 105
Velez, C. E. 1974, CeMec, 10, 405
Velez, C. E., & Hilinski, S. 1978, CeMec, 17, 83